A Fully Human Antimelanoma Cellular Adhesion Molecule/MUC18 Antibody Inhibits Spontaneous Pulmonary Metastasis of Osteosarcoma Cells *In Vivo*

Eric C. McGary,[1] Amy Heimberger,[2] Lisa Mills,[1] Kristy Weber,[1] Gary W. Thomas,[3] Mikhail Shtivelband,[4] Dina Chelouche Lev,[1] and Menashe Bar-Eli[1,6]

Departments of [1]Cancer Biology and [2]Neurosurgery, The University of Texas M. D. Anderson Cancer Center, Houston, Texas; [3]Hilton Head Regional Medical Center, Hilton Head, South Carolina; and [4]The University of Texas Medical School, Department of Hematology, Houston, Texas

ABSTRACT

Purpose: **The melanoma cellular adhesion molecule, also known as MUC18, is highly expressed on several tumors, including bone sarcomas. The level of MUC18 expression has been found to correlate directly with tumor progression and metastatic potential. These observations have established MUC18 as a candidate mediator of tumor growth and metastasis, and suggest that blockade of MUC18 might be a potential target for immunotherapy against several MUC18-expressing tumors, including human bone sarcomas.**

Experimental Design: **To investigate whether blockade of MUC18 might be a potential target for immunotherapy against osteosarcoma, we have recently developed a fully human anti-MUC18 antibody, ABX-MA1. We studied the effect of ABX-MA1 on growth, adhesion, invasion, and metastasis of human osteosaroma cells both *in vitro* and *in vivo*.**

Results: **MUC18 was widely expressed on both osteosarcoma and Ewing's sarcoma cells. ABX-MA1 had no effect on the proliferation of osteosarcoma cells *in vitro*, nor did it significantly inhibit the growth of KRIB human osteosarcoma cells when they were orthotopically implanted into the tibias of nude mice. However, after 6 weeks, significantly fewer ABX-MA1-treated mice developed spontaneous pulmonary metastases than did IgG-treated control mice. Additionally, ABX-MA1 decreased the invasion of osteosarcoma cells through Matrigel-coated filters and disrupted homotypic adhesion between osteosarcoma cells and their heterotypic interaction with human vascular endothelial cells.**

Conclusions: **Our findings demonstrate that MUC18 plays a central role in the metastasis of osteosarcoma and suggest that targeted inhibition of this antigen by ABX-MA1 may be a novel immunotherapeutic approach in the management of this tumor.**

INTRODUCTION

Osteosarcoma is the most common primary malignant bone tumor in children. Clinically evident metastatic disease is present in 10–20% of patients at diagnosis. Despite advancements in multimodality treatment, 5-year survival rates approximate 40–50% (1). At the time of diagnosis, microscopic dissemination is present in as many as 80% of children with bone sarcomas. The observed improvement in 5-year survival rate has been attributed to the eradication of microscopic disease with adjuvant or neoadjuvant chemotherapy. However, improvements in these therapies are needed, because relapse with distant metastases is a persistent problem and is associated with limited treatment options.

Cellular adhesion molecules (CAMs) are expressed on the cell surface, and play important roles in organogenesis, tissue homeostasis, wound healing, and inflammatory and immune responses (2). The melanoma CAM (MCAM), also known as MUC18, Mel-CAM, CD146, A32 antigen, and S-Endo-1, is a membrane glycoprotein that functions as a Ca^{2+}-independent adhesion molecule. MUC18 was originally cloned and sequenced from a melanoma cDNA library (3). The molecule contains the characteristic V-V-C2-C2-C2 immunoglobulin-like domain structure and belongs to the immunoglobulin superfamily (4). The MUC18 cytoplasmic domain contains several protein kinase recognition motifs, suggesting the involvement of this molecule in cell signaling. The gene encoding MUC18 is located on human chromosome 16 and encodes a glycosylated protein with a molecular weight of M_r ~113,000 (5).

Although MUC18 is principally expressed on malignant melanoma and rarely on melanocytes or benign lesions, it is now recognized that it is also expressed on various other normal and malignant tissues (6). MUC18 expression is consistently present on other tumors such as angiosarcomas, Kaposi's sarcomas, leiomyosarcomas, placental site trophoblastic tumors, and choriocarcinomas (7, 8). It is also expressed in normal adult tissues, including but not limited to smooth muscle, endothelium, mammary ductal/lobular epithelium, and adult peripheral nerve tissue (9).

MUC18 has been studied extensively in malignant melanoma, partly because of the well-described sequential progression of the disease and characterization of CAMs expressed at

Received 7/2/03; revised 9/2/03; accepted 9/8/03.
Grant support: NIH training grant T-32-09666 (E. C. M.), The University of Texas M. D. Anderson Cancer Center Department of Cancer Medicine, and NIH Grant CA 76098.
Notes: Drs. McGary and Heimberger contributed equally to this work. The costs of publication of this article were defrayed in part by the payment of page charges. This article must therefore be hereby marked *advertisement* in accordance with 18 U.S.C. Section 1734 solely to indicate this fact.
Requests for reprints: Menashe Bar-Eli, Department of Cancer Biology, Unit-173, The University of Texas M. D. Anderson Cancer Center, 7777 Knight Road, Houston, TX 77054. Phone: (713) 794-4004; Fax: (713) 792-8747; E-mail: mbareli@mdanderson.org.

each step (10–12). Approximately 70% of melanoma metastases express MUC18 and, among primary tumors, its expression increases with increasing vertical thickness, an important predictor of metastatic disease (13). Indeed, the expression of MUC18 by melanoma cell lines correlates with their ability to grow and produce metastases *in vivo*. This hypothesis is supported by the observation that the production of tumorigenic variants from a nontumorigenic melanoma cell line is accompanied by MUC18 up-regulation and by the observation that enforced MUC18 expression in primary cutaneous melanoma leads to increased tumor growth and metastasis *in vivo* (14, 15).

Taken together, these findings have defined MUC18 as a candidate for mediating tumor growth and metastasis, and also lend credence to the rationale that blocking MUC18 might be a potential target for immunotherapy against several MUC18-expressing tumors. Indeed, we have demonstrated previously that fully human antibodies to MCAM/MUC18 (ABX-MA1) inhibited tumor growth and metastasis of human melanoma in nude mice (16). In this study, we show for the first time that MUC18 is expressed on osteosarcoma cells. In addition, we demonstrate inhibition of metastasis of human osteosarcoma cells *in vivo* through functional blockade of MUC18 by ABX-MA1. Disruption of homotypic and heterotypic cellular adhesions by ABX-MA1 may in part explain its ability to inhibit tumor cell metastasis. These results suggest that blocking MCAM/MUC18 with ABX-MA1 could be beneficial for treatment of patients with osteosarcoma either when used alone or in combination with chemotherapeutic agents.

MATERIALS AND METHODS

Cell Lines. TE-85 osteosarcoma and TC-71 Ewing's sarcoma cell lines were kindly provided by Dr. Z. Zhou (The University of Texas M. D. Anderson Cancer Center, Houston, TX). MNNG-HOS (Cl #5), Saos-2, and MG-63 osteosarcoma cells were obtained from the American Type Culture Collection (Manassas, VA). The KRIB osteosarcoma cell line was kindly provided by Dr. P. Choong (Melbourne, Australia). Pooled human umbilical vein endothelial cells (HUVECs) were obtained from Clonetics (Rockland, ME) and cultured in MCBD-13 medium (Clonetics). A375SM and SB-2 melanoma cells were established from human melanoma specimens (16). Cells were grown in 10% FCS and MEM made complete by the addition of glutamine, HEPES, streptomycin, nonessential amino acids, and multivitamins. All of the cells were incubated at 37°C in conditions of 5% CO_2/95% air.

ABX-MA1. ABX-MA1 is a human IgG2 monoclonal antibody generated against human MUC18 using Abgenix (Fremont, CA) proprietary XenoMouse mice. In XenoMouse technology, murine heavy and κ chain loci have been inactivated and subsequently replaced with a majority of human heavy and light κ light chain immunoglobulin loci. When immunized, these mice produce fully human antibodies (17). The mice used contained only the human IgG2 heavy chain sequences and human κ light chain. Chemically pure human IgG control antibody was purchased from Jackson ImmunoResearch Laboratories (West Grove, PA) and used at the same concentration as ABX-MA1 for all of the studies.

Western Blot Analysis. Osteosaroma and Ewing's sarcoma cells were seeded at 1×10^6 in 100-mm tissue culture plates in 10 ml of complete MEM. After overnight incubation, the cells were washed with ice-cold PBS solution and lysed in 0.2 ml of lysis buffer (Cell Signaling Technologies, Beverly, MA) at 4°C for 30 min. Lysates were cleared by a 10-min centrifugation at 10,000 × *g*, and protein determination was carried out according to the method of Bradford (18). Samples were subjected to 7.5% PAGE analysis after they were boiled for 5 min in sample buffer containing SDS. The separated proteins were transferred to Immobilon-P membranes (Millipore, Bedford, MA) and then blocked for 1 h in Tris-buffered saline plus Tween 20 (1× Tris buffered saline +0.1% Tween 20) containing 5% nonfat milk. The membranes were then incubated with either ABX-MA1 or control IgG antibody (1:500 dilution) overnight. Membranes were probed with secondary antibody peroxidase-conjugated AffiniPure rabbit antihuman IgG (H + L) for 1 h and then washed twice with Tris-buffered saline plus Tween 20. Bound antibody was detected using ECL reagent (Amersham Pharmacia, Piscataway, NJ). Equal loading of protein samples was confirmed by incubating membranes with a primary antibody specific for actin (Santa Cruz Biotechnology, Santa Cruz, CA).

Proliferation Assay. Proliferation of KRIB cells was assessed on day 0 (treatment day) through day 5 in the presence of ABX-MA1 or control IgG antibody. Proliferation was assayed by the 3-(4,5-dimethylthiazol-2-yl)-2,5-diphenyltetrazolium bromide dye technique, which relies on the metabolic reduction of the tetrazolium salt 3-(4,5-dimethylthiazol-2-yl)-2,5-diphenyltetrazolium bromide by living cells. 3-(4,5-Dimethylthiazol-2-yl)-2,5-diphenyltetrazolium bromide (40 μg) was added to each well, and the cells were incubated at 37°C for 2 h, after which DMSO was added; 15 min after the addition of DMSO, we determined the absorbance using an automated dual-wavelength spectrophotometer (Bio-Tek Instruments, Winooski, VT) against a reagent blank at a test wavelength of 570 nm and a reference of 630 nm. Absorbance was determined with a microplate reader.

Three-Dimensional Spheroid Culture. Multicellular spheroids were generated by the liquid overlay technique (19, 20). Twenty-four well tissue culture plates were coated with 250 μl of 1% SeaPlaque agarose (FMC Bioproducts, Rockland, ME) solution in serum-free MEM. A single suspension of 1×10^5 A375SM, SB-2 (melanoma cell lines, MUC18-positive and -negative, respectively), TC-71, or KRIB cells were diluted in 25 μl of hybridoma medium, plated with 475 μl of control IgG (1:200 dilution) or ABX-MA1, and incubated at 37°C in 5% CO_2. After 24 h, we determined spheroid formation. Images were captured by bright-field microscopy and photographed in digital format.

Attachment of Bone Sarcoma Cells to HUVECs. Attachment of bone sarcoma cells to HUVECs treated with 12 μg/ml IgG or ABX-MA1 was measured by plating 4×10^4 HUVEC in 96-well plates and allowing them to attach to the plates for 24 h. A thin overlay of 2% BSA was placed in each well and incubated overnight at 37°C. Five $\times 10^4$ treated, or untreated KRIB or TC-71 cells were added to each well and incubated overnight at 37°C. Wells were washed twice with PBS, and cells in each well were counted. Results are presented

as the percentage of cells adhered from the total number of cells seeded.

Invasion Assay through Matrigel. Invasion of KRIB and LM8 cells was measured by plating 2.5×10^3 cells in six-well plates. After 24 h, the cells were treated with 100 μg/ml ABX-MA1 or control IgG for 5 days. Treatment for 5 days was found to be optimal for the antibody to affect invasion through Matrigel. Cells were then treated with trypsin-EDTA and counted. Biocoat Matrigel invasion chambers (Becton-Dickinson, Franklin Lakes, NJ) were primed according to the manufacturer's directions, and then 20% MEM was placed in the lower chamber to act as a chemoattractant. KRIB or LM8 cells (2.5×10^3 in 500 μl of serum-free medium) were placed in the upper chamber with ABX-MA1 or IgG control antibody. Cells were incubated at 37°C for 22 h. Cells on the lower surface of the filter were stained with Diff-Quick (American Scientific Products, McGraw Park, IL) and quantified with an image analyzer (Optimas 6.2) attached to an Olympus CK2 microscope. The data were expressed as the mean number of cells from 10 high-power fields that migrated to the lower surface of the filter in each of three experiments performed.

Intratibial Implantation of KRIB Cells into Nude Mice. Female athymic nude mice were purchased from the Animal Production Area of the National Cancer Institute's Frederick Cancer Research Facility (Frederick, MD) and maintained in specific-free-pathogen animal facilities approved by the American Association for Accreditation of Laboratory Animal Care. They were used for experiments when they were 9 weeks old.

Cultured KRIB cells (80% confluence) were harvested for use in intratibial injections after a brief exposure to 0.25% trypsin and 0.02% EDTA. Trypsinization was stopped after 2 min with medium containing 10% fetal bovine serum, and the cells were washed once in serum-free medium and resuspended in HBSS. Only suspensions consisting of single cells with >90% viability were used for the injections. The cells (5×10^4 cells/mouse) were injected into the right tibias of nude mice anesthetized with sodium pentobarbital (50 mg/kg i.p.). To evaluate them for the presence of bone lesions, the mice were anesthetized weekly beginning 3 weeks after tumor cell injection; tumor growth was monitored by radiographic imaging with a Faxitron MX-20 X-ray unit (Wheeling, IL) and the images captured digitally. The experiment was ended when marked tibial bone destruction with a soft tissue extension of the tumor occurred in the control animals.

Therapy of Osteosarcoma Cells Growing in the Tibias of Nude Mice. Three days after the KRIB cells were injected intratibially into the nude mice, they were randomly allocated to two treatment groups ($n = 19$ each): one group received i.p. injections of ABX-MA1 (100 μg) three times weekly, and the other, i.p. injections of control IgG antibody three times weekly. After 45 days of treatment, mice were humanely killed by exposure to carbon dioxide, and their body weights were determined. The right tibia from mice treated with ABX-MA1 ($n = 5$) and mice treated with control IgG antibody ($n = 5$) was harvested, processed, and weighed. The lungs from all of the ABX-MA1-treated mice ($n = 19$) and control mice ($n = 19$) were harvested and processed. Sections of the lungs were stained with H&E and examined for the presence of spontaneous micrometastases. Histopathologic examination confirmed the nature of the disease.

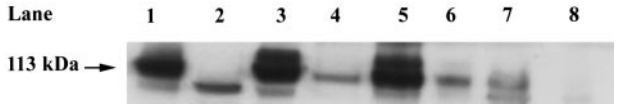

Fig. 1 MUC18 expression on human bone sarcoma cells. Fully human anti-MUC18 antibody (ABX-MA1) detected a band of M_r 113,000 MUC18 protein on the metastatic (MUC18-positive) melanoma cell line A375SM (positive control, *Lane 1*). The M_r 113,000 MUC18 band was not detected on the MUC18-negative SB-2 cell line (negative control, *Lane 2*), but it was observed on four of the five osteosarcoma cell lines tested: TE-85 (*Lane 3*), Saos-2 (*Lane 5*), MNNG/HOS (*Lane 6*), and KRIB (*Lane 7*). MUC18 was also detected on a Ewing's sarcoma cell line (TC-71, *Lane 4*). One of the five osteosarcoma cell lines tested (MG-63, *Lane 8*) did not express detectable levels of MUC18. Equal loading of the gel was confirmed by β-actin expression (data not shown).

Statistical Analysis. *In vitro* data were analyzed for significance by using the two-tailed Student *t* test, and the *in vivo* data were analyzed by using Wilcoxon's rank-sum test.

RESULTS

Generation of Specific Fully Human Anti-MUC18 (ABX-MA1). XenoMouse mice were immunized with SK-Mel28 cells, which express high levels of MUC18, and boosted with SK-Mel28 cells admixed with soluble MUC18-human IgG2 Fc fusion protein. B cells derived from the spleen and lymph nodes were fused with myeloma P3X63Ag8.653. From the resulting hybridoma supernatants, the ABX-MA1 clone was selected on the basis of its ability to bind soluble MUC18 antigen. ABX-MA1 detected a band corresponding to the M_r 113,000 MUC18 protein in the metastatic melanoma cell line A375SM (Refs. 14, 20; Fig. 1, *Lane 1*). The specificity of ABX-MA1 was additionally confirmed by the inability to detect the dominant M_r 113,000 MUC18 protein on the MUC18-negative SB-2 melanoma cell line (Ref. 16; Fig. 1, *Lane 2*). The band of lower molecular weight may represent a nonspecific band or possibly a precursor to MUC18, which has not been fully glycosylated and transported to the cell surface. The later is supported by our prior studies in which we used fluorescence-activated cell sorter analysis to demonstrate the presence and absence of MUC18 expression on A375SM and SB-2 cells, respectively (16).

MUC18 Is Widely Expressed on Bone Sarcoma Cells. Expression of MUC18 on four of the osteosarcoma cell lines and the Ewing's sarcoma cell line was determined by Western blotting with ABX-MA1 (Fig. 1). MUC18 levels were high in TE-85 and Saos-2 cells (Fig. 1, *Lanes 3* and *5*) and were moderate in TC-71, KRIB, and MNNG-HOS cells (Fig. 1, *Lanes 4*, *6*, and *7*). MUC18 was not detectable on one of the other osteosarcoma cell lines, MG-63 (Fig. 1, *Lane 8*). Only those cells expressing MUC18 were selected for additional studies. Although the expression of MUC18 on KRIB osteosarcoma cells was less than that on other osteosarcoma cell lines, KRIB cells were selected for additional studies because of their ability to spontaneously metastasize to the lungs after having been orthotopically implanted into the tibia of nude mice.

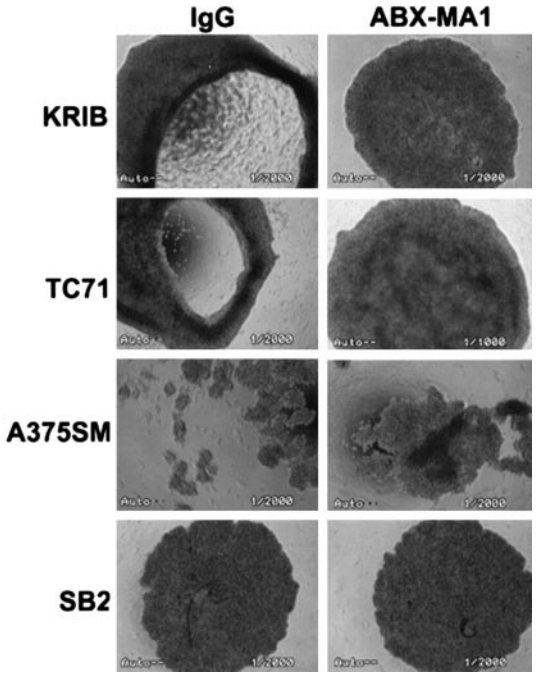

Fig. 2 Disruption of spheroid formation by fully human anti-MUC18 antibody (*ABX-MA1*). ABX-MA1, but not control IgG antibody, blocked spheroid formation in MUC18-positive KRIB, TC-71, and A375SM cells. The MUC18-negative melanoma cell line, SB-2, was used as a negative control; neither ABX-MA1 nor control IgG antibody had any effect on SB-2 cell line.

ABX-MA1 Inhibits Homotypic Interaction between Bone Sarcoma Cells. Homotypic interactions between tumor cells may play a role in tumor cell extravasation by supporting tumor cell survival in the vasculature and arrest in small vessels. Therefore, we studied the effect of ABX-MA1 on homotypic interactions among bone sarcoma cells using a three-dimensional culture system (19, 20). Using this system, adherence and formation of monolayers by the cells are prevented by the presence of a thin layer of solid agarose, forcing the cells to form tumor-like homotypic multicellular aggregates (14, 16). When either MUC18-positive KRIB or TC-71 bone sarcoma cells were cultured in the presence of control IgG, the cells formed three-dimensional multicellular aggregates (Fig. 2, IgG panels). When the cells were cultured with ABX-MA1 (added at time 0), spheroid formation was disrupted (Fig. 2, ABX-MA1 panels). Similarly, in the presence of IgG, MUC18-positive A375SM cells formed three-dimensional multiaggregates. However, in the presence of ABX-MA1, A375-SM cells grew in a one-dimensional monolayer indicating disruption of homotypic adhesion (Fig. 2, A375SM panels). MUC18-negative SB-2 cells did not form multicellular aggregates but rather grew in monolayers in the presence of IgG. This finding suggests the lack of homotypic interactions among MUC18-negative cells. Addition of ABX-MA1 to MUC18-negative cells had no effect on the monolayer (Fig. 2, SB-2 panels). This assay confirms the ability of ABX-MA1 to inhibit homotypic aggregation among bone sarcoma cells expressing the MUC18 CAM.

ABX-MA1 Inhibits Heterotypic Interactions between Bone Sarcoma Cells and Endothelial Cells. As is the case with homotypic interactions, heterotypic interactions may play a central role in the metastatic cascade. Heterotypic interactions between bone sarcoma cells and endothelial cells may augment tumor cell intravasation and extravasation. Because HUVECs express MUC18 (16), we next determined whether ABX-MA1 could inhibit the homotypic interaction between bone sarcoma cells and HUVECs. Fig. 3 demonstrates that both TC-71 and KRIB cells attached to HUVECs. Treatment with ABX-MA1, but not with control IgG antibody, inhibited TC-71- and KRIB-HUVEC interaction (Fig. 3). A quantitative summary performed on the attachment of bone sarcoma cells to HUVECs demonstrates that ABX-MA1 inhibited adhesion of KRIB and TC-71 cells to HUVECs by 70% and 65%, respectively (two-tailed $P < 0.01$ for both comparisons). These data provide an additional mechanism by which ABX-MA1 may inhibit tumor extravasation and metastasis through the inhibition of heterotypic interactions between bone sarcoma cells and HUVECs.

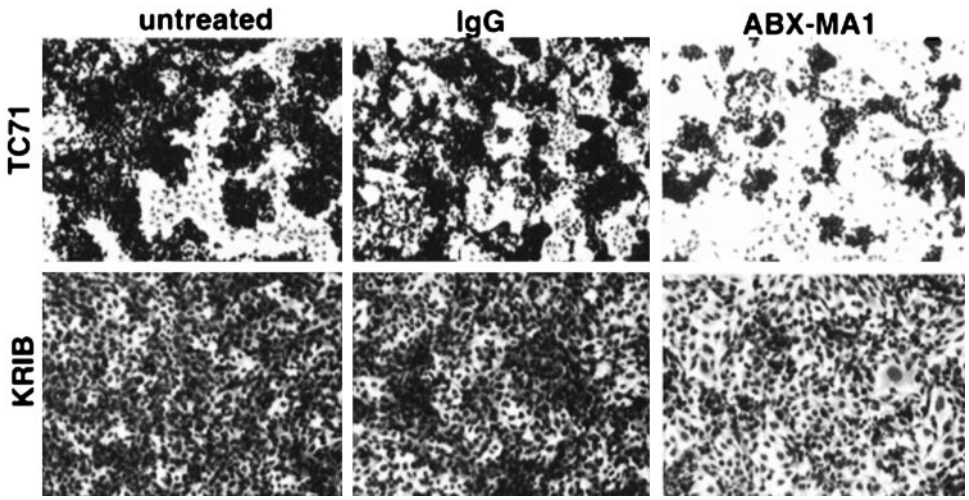

Fig. 3 Effect of fully human anti-MUC18 antibody (*ABX-MA1*) on attachment of osteosarcoma and Ewing's sarcoma cells to human umbilical vein endothelial cells (HUVECs). The KRIB osteosarcoma and TC-71 Ewing's sarcoma cell lines were cocultured with HUVECs in the presence of ABX-MA1 or control IgG antibody. In both cell lines, the endothelial cell-sarcoma cell heterotypic interaction was inhibited by ABX-MA1 but not by control IgG antibody.

Effect of ABX-MA1 on Osteosarcoma Cell Invasion *in Vitro*. We next analyzed whether ABX-MA1 could inhibit the invasion of osteosarcoma cells through Matrigel-coated filters. To that end, 2.5×10^3 LM8 and KRIB osteosarcoma cells that had been treated with either ABX-MA1 (100 μg/ml) or control IgG antibody for 5 days were placed in the upper compartment of an invasion chamber in the presence of either ABX-MA1 (100 μg/ml) or IgG antibody. After 22 h, the cells on the lower surface were counted. Osteosarcoma cells treated with ABX-MA1 exhibited significantly less invasion than did IgG-treated cells (two-tailed $P < 0.0001$ for both comparisons; Table 1). These results indicate that blockade of MUC-18 by ABX-MA1 inhibits the ability of osteosarcoma cells to penetrate the basement membrane, an important step in tumor intravasation and extravasation.

ABX-MA1 Inhibits Spontaneous Metastasis of KRIB Osteosarcoma Cells *In Vivo*. An animal model of osteosarcoma has been established using the KRIB cell line. When KRIB cells are orthotopically transplanted into the tibias of congenitally athymic nude mice, bone tumors that are histologically and radiographically similar to human primary osteosarcomas develop within 4 weeks. Furthermore, most of the mice with viable xenografts subsequently develop pulmonary metastasis (21).

To study the effect of ABX-MA1 on osteosarcoma growth *in vivo*, 5×10^4 KRIB cells were injected into the tibias of 38 athymic nude mice. After 3 days, the mice were randomly allocated to two treatment groups ($n = 19$ each): one group received i.p. injections of ABX-MA1 (100 μg) three times weekly, and the other, i.p. injections of control IgG antibody, three times weekly.

After 45 days of treatment, mice were humanely killed, and the incidence of primary tumors that had developed in the tibias was determined. The number of mice that developed tibial tumors was similar in both treatment groups [16 mice (84%) in IgG-treated mice and 15 mice (79%) in the ABX-MA1-treated group; Table 2]. Five mice that had developed primary bone tumors were randomly selected from each treatment group, and each tumor-bearing was weighed. The mean tibial weight was lower in mice treated with ABX-MA1 (mean, 550 mg; range, 385–977 mg) than in those treated with control IgG (mean, 788 mg; range, 631–988 mg; $P = 0.088$). Although the trend was toward smaller tumors in the treatment group as determined by mean tibial weight, this did not reach statistical significance.

Table 1 Invasion of ABX-MA1[a]-treated osteosarcoma cells through Matrigel-coated filters

Data are shown as mean numbers of cells (±SD) from 10 high-powered fields in three experiments.

Cell line	Treatment	No. of migrated cells ± SD	Invasion (%)	P^b
KRIB	IgG antibody	1937 ± 40	73	
KRIB	ABX-MA1	993 ± 25	23	<0.0001
LM8	IgG antibody	1219 ± 19	74	
LM8	ABX-MA1	429 ± 13	24	<0.0001

[a] ABX-MA1, fully human anti-MUC 18 antibody.
[b] As determined by Wilcoxon's rank-sum test.

Table 2 Spontaneous lung metastasis of KRIB cells in nude mice after treatment with ABX-MA1[a]

Treatment	Primary bone tumors	Spontaneous lung metastases	Incidence of lung metastases from bone tumors[b]
IgG antibody	16/19 (84%)	12/19 (63%)	12/16 (75%)
ABX-MA1	15/19 (79%)	2/19 (11%)[c]	2/15 (13%)[b]

[a] ABX-MA1, fully human anti-MUC18 antibody.
[b] The incidence of lung metastasis occurring in mice with established bone tumors.
[c] $P < 0.0001$ versus IgG-treated animals, as determined by Wilcoxon's rank-sum test.

This may have been because of the small sample size ($n = 5$ for both treatment and control groups) and the large SD.

The incidence of spontaneous metastasis was significantly less in ABX-MA1-treated mice than it was in IgG-treated control mice, 2 (11%) *versus* 12 (63%; Wilcoxon's rank-sum $P < 0.0001$ for both comparisons; Table 2). In the ABX-MA1-treated group, of the two mice that developed pulmonary metastases, one developed a single microscopic metastases and the second mouse developed five microscopic metastases. In the IgG-treated group, of the 12 mice that developed pulmonary metastases, all developed at least one but not more than two microscopic metastases. Fig. 4 illustrates the presence and absence of spontaneous lung metastasis (as determined by H&E staining) in a representative control mouse and an ABX-MA1-treated mouse, respectively. Because spontaneous lung metastases occur only in mice that have established tumors from intratibially xenografted KRIB cells, the incidence of lung metastasis occurring in mice with established bone tumors was 2 of 15 (13%) in ABX-MA1-treated mice and 12 of 16 (75%) in IgG-treated mice (Wilcoxon's rank-sum $P < 0.0001$ for both comparisons; Table 2).

These results demonstrate that ABX-MA1 inhibited spontaneous pulmonary metastasis in mice bearing intratibial KRIB osteosarcoma xenografts, but not tumorigenicity, as determined by the weight of tumor-bearing tibias.

DISCUSSION

Tumor progression and metastasis depends on factors intrinsic to the tumor cells, including growth factors and their cognate receptors, extracellular matrix proteins, proteases, chemokines, and CAMs. In this study, we have demonstrated that blockade of the CAM, MUC18, inhibits metastasis of bone sarcomas *in vivo*.

Malignant melanoma has served as an excellent model for studying CAMs, partly because it has a sequential series of five definable stages. As the malignant phenotype of melanoma cells change from the noninvasive radial growth phase to the vertical growth phase, which has high metastatic potential, so does the repertoire of the CAMs expressed on the surface of the cells. MUC18 confers metastatic potential and increased tumorigenicity to melanoma cells and is expressed in high levels on the cell surface (6, 13). Although the expression of MUC18 has been demonstrated on several tumors other than melanoma, including sarcomas (7, 8), we are unaware of any other studies showing its expression on human osteosarcoma and Ewing's sarcoma cells.

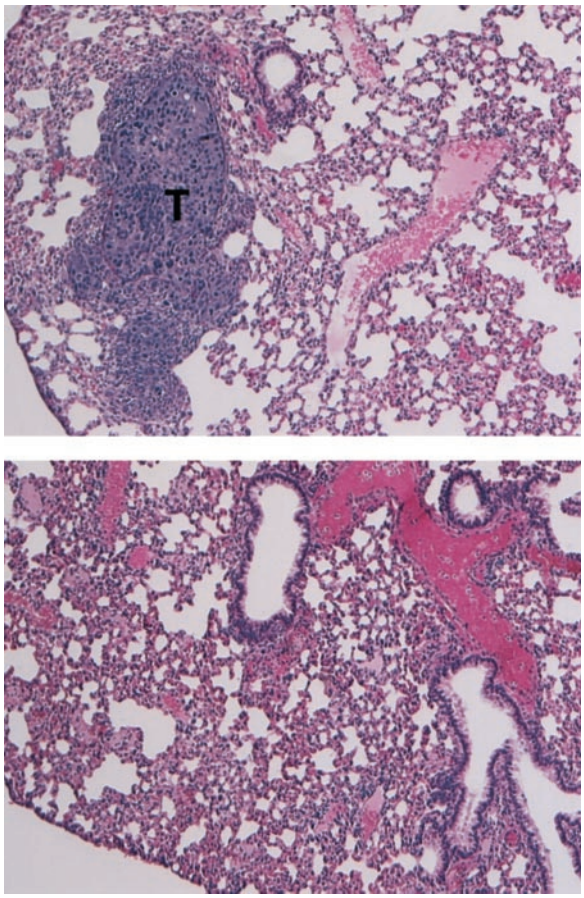

Fig. 4 Effect of fully human anti-MUC18 antibody (ABX-MA1) on metastasis of human osteosarcoma cells in athymic nude mice. KRIB (5×10^4) cells were orthotopically implanted into the tibias of 38 nude nice. Three days later, the mice were treated for 45 days with ABX-MA1 (100 mg i.p., three times weekly; $n = 19$) or control IgG antibody (100 μg i.p., three times weekly; $n = 19$). Cross-sections of paraffin-embedded lung tissue demonstrate the histological presence (*top*; T = tumor) and absence (*bottom*) of spontaneous lung metastases from a representative IgG-treated and an ABX-MA1-treated mouse, respectively (H&E staining).

Indeed, most of the bone sarcomas we tested expressed high levels of MUC18; TE-85 and Saos-2 osteosarcoma cells expressed levels comparable with those of the highly metastatic A375SM melanoma cells.

To study the effect of ABX-MA1 on tumor growth and metastasis *in vivo*, we sought a tumor model that would parallel the natural course of osteosarcoma in humans. Samid and Mandler (22) established and characterized the v-Ki-ras-transformed human osteosarcoma cell line KRIB. Although KRIB cells expressed lower levels of MUC18 than the other cell lines, we studied them further because they have intrinsic properties that make them an excellent tumor model *in vivo*. What makes this cell line an especially useful model is that when they are orthotopically implanted into the tibias of athymic mice, interosseous tumors develop that are histologically and radiographically indistinguishable from human bone osteosarcomas.

ABX-MA1 had no effect on tumor cell proliferation *in vitro* [3-(4,5-dimethylthiazol-2-yl)-2,5-diphenyltetrazolium bromide assay; data not shown], and did not affect the tumorigenicity of KRIB cells after they had been orthotopically implanted into the tibia of nude mice. However, ABX-MA1 significantly inhibited spontaneous metastasis of KRIB cells *in vivo*. Homotypic adhesion between bone sarcoma cells may play an important part in the metastatic cascade by promoting tumor cell aggregation and arrest in small vessels. Our results show that in the absence of ABX-MA1, KRIB osteosarcoma and TC-71 Ewing's sarcoma cells form well-organized homotypic aggregates. It was interesting that unlike the tumor aggregates formed in MUC18-expressing melanoma cells, those formed among bone sarcoma cells appear to be highly organized, taking on an elliptical form. In the presence of ABX-MA1, however, this complex cytoskeletal architecture is severely disrupted. These data suggest that the loss in homotypic adhesion mediated by ABX-MA1 disrupts the cytoskeletal network of the primary tumor. Loss of homotypic interactions between tumor cells may inhibit tumor cell aggregation and arrest in small vessels. This may partly explain why mice treated with ABX-MA1 developed fewer pulmonary metastases than were observed in mice treated with control IgG antibody.

The KRIB osteosarcoma model provides a unique advantage for studying tumor cell metastasis *in vivo*: because these cells spontaneously metastasize to the lungs from the primary tumor xenograft, which is consistent with the normal progression of osteosarcoma in humans (21), the entire metastasis cascade from tumor cell disassociation to organ invasion can be studied. Our data demonstrated that ABX-MA1, compared with IgG antibody, significantly inhibited spontaneous lung metastasis from the primary xenograft. CAMs have been shown to play an important role in the dynamic process of transendothelial migration (23). Indeed, heterotypic interactions between MUC18-expressing tumors and MUC18-expressing HUVECs have been demonstrated (20), suggesting that such interactions may play a central role in the process of tumor-cell intravasation and extravasation late in the metastatic cascade. Our data showed that ABX-MA1 inhibits heterotypic bone sarcoma-endothelial cell interaction, which may additionally explain the dramatic decrease in spontaneous lung metastasis observed in mice treated with ABX-MA1. However, unlike the case with experimental metastasis models that study the later steps of the metastatic cascade, with this model it is not possible to determine whether the inhibition of metastasis by ABX-MA1 was attributable to tumor-cell disassociation (*i.e.*, a homotypic disruption) or to inhibition of intravasation and extravasation (*i.e.*, a disruption of heterotypic interaction with endothelial cells). Furthermore, we demonstrated that cells treated with ABX-MA1 exhibited impaired invasion through Matrigel-coated filters. We have shown previously that MUC18 contributes to the metastatic phenotype of melanoma cells through the induction of matrix metalloproteinase-2 (14). As expected, these MUC18-expressing cells exhibited increased invasion through Matrigel-coated filters compared with MUC18-negative cells. ABX-MA1 inhibited the invasion of melanoma cells through Matrigel-coated filters via inhibition of matrix metalloproteinase-2 expression (16).

Taken together, our data demonstrate that ABX-MA1 inhibits the metastasis of osteosarcoma *in vivo*. The MUC18

cytoplasmic domain contains several protein kinase recognition motifs, suggesting the involvement of MUC18 in cell signaling. Although our *in vitro* data provide mechanistic insights into the antitumor activity of ABX-MA1, we cannot rule out the possibility that ABX-MA1 could, in part, mediate its effect through inhibition of MUC18 cell-signaling pathways that remain to be elucidated. In addition, we cannot rule out the possibility that ABX-MA1 could activate murine complement or mediate antibody-dependent cell cytotoxicity with murine monocytes through the Fc portion of the antibody. We are investigating these possibilities. ABX-MA1 is currently in early stage clinical trials for the treatment of malignant melanoma; our data suggest that ABX-MA1 may also be a novel immunotherapeutic approach to the treatment of osteosarcoma as either adjuvant or neoadjuvant therapy.

ACKNOWLEDGMENTS

We thank Dr. Kevin Raymond, Karen Phillips, Michelle Doucet, and Carol Oborn for technical assistance.

REFERENCES

1. Bramwell, V. H. The role of chemotherapy in the management of non-metastatic operable extremity osteosarcoma. Semin. Oncol., *24:* 561–571, 1997.

2. Koukoulis, G. K., Patriarca, C., and Gould, V. E. Adhesion molecules and tumor metastasis. Hum. Pathol., *29:* 889–892, 1998.

3. Lehmann, J. M., Riethmuller, G., and Johnson, J. P. MUC18, a marker of tumor progression in human melanoma, shows sequence similarity to the neural cell adhesion molecules of the immunoglobulin superfamily. Proc. Natl. Acad. Sci. USA, *86:* 9891–9895, 1989.

4. Holness, C. L., and Simmons, D. L. Structural motifs for recognition and adhesion in members of the immunoglobulin superfamily. J. Cell Sci., *107:* 2065–2070, 1994.

5. Sers, C., Kirsch, K., Rothbacher, U., Riethmuller, G., and Johnson, J. P. Genomic organization of the melanoma-associated glycoprotein MUC18: implications for the evolution of the immunoglobulin domains. Proc. Natl. Acad. Sci. USA, *90:* 8514–8518, 1993.

6. Lehmann, J. M., Holzmann, B., Breitbart, E. W., Schmiegelow, P., Riethmuller, G., and Johnson, J. P. Discrimination between benign and malignant cells of melanocytic lineage by two novel antigens, a glycoprotein with a molecular weight of 113, 000 and a protein with a molecular weight of 76, 000. Cancer Res., *47:* 841–845, 1987.

7. Shih, I. M., Nesbit, M., Herlyn, M., and Kurman, R. J. A new Mel-CAM (CD146)-specific monoclonal antibody, MN-4, on paraffin-embedded tissue. Mod. Pathol., *11:* 1098–1106, 1998.

8. Shih, I. M., Wang, T. L., and Westra, W. H. Diagnostic and biological implications of mel-CAM expression in mesenchymal neoplasms. Clin. Cancer Res., *2:* 569–575, 1996.

9. Shih, I. M., Elder, D. E., Speicher, D., Johnson, J. P., and Herlyn, M. Isolation and functional characterization of the A32 melanoma- associated antigen. Cancer Res., *54:* 2514–2520, 1994.

10. Nesbit, M., and Herlyn, M. Adhesion receptors in human melanoma progression. Invasion Metastasis, *14:* 131–146, 1994.

11. Elder, D. E., Rodeck, U., Thurin, J., Cardillo, F., Clark, W. H., Stewart, R., and Herlyn, M. Antigenic profile of tumor progression stages in human melanocytic nevi and melanomas. Cancer Res., *49:* 5091–5096, 1989.

12. Elder, D. E., Clark, W. H., Jr., Elenitsas, R., Guerry, D. t., and Halpern, A. C. The early and intermediate precursor lesions of tumor progression in the melanocytic system: common acquired nevi and atypical (dysplastic) nevi. Semin. Diagn. Pathol., *10:* 18–35, 1993.

13. Holzmann, B., Brocker, E. B., Lehmann, J. M., Ruiter, D. J., Sorg, C., Riethmuller, G., and Johnson, J. P. Tumor progression in human malignant melanoma: five stages defined by their antigenic phenotypes. Int. J. Cancer, *39:* 466–471, 1987.

14. Xie, S., Luca, M., Huang, S., Gutman, M., Reich, R., Johnson, J. P., and Bar-Eli, M. Expression of MCAM/MUC18 by human melanoma cells leads to increased tumor growth and metastasis. Cancer Res., *57:* 2295–2303, 1997.

15. Bani, M. R., Rak, J., Adachi, D., Wiltshire, R., Trent, J. M., Kerbel, R. S., and Ben-David, Y. Multiple features of advanced melanoma recapitulated in tumorigenic variants of early stage (radial growth phase) human melanoma cell lines: evidence for a dominant phenotype. Cancer Res., *56:* 3075–3086, 1996.

16. Mills, L., Tellez, C., Huang, S., Baker, C., McCarty, M., Green, L., Gudas, J. M., Feng, X., and Bar-Eli, M. Fully human antibodies to MCAM/MUC18 inhibit tumor growth and metastasis of human melanoma. Cancer Res., *62:* 5106–5114, 2002.

17. Mendez, M. J., Green, L. L., Corvalan, J. R., Jia, X. C., Maynard-Currie, C. E., Yang, X. D., Gallo, M. L., Louie, D. M., Lee, D. V., Erickson, K. L., Luna, J., Roy, C. M., Abderrahim, H., Kirschenbaum, F., Noguchi, M., Smith, D. H., Fukushima, A., Hales, J. F., Klapholz, S., Finer, M. H., Davis, C. G., Zsebo, K. M., and Jakobovits, A. Functional transplant of megabase human immunoglobulin loci recapitulates human antibody response in mice. Nat. Genet., *15:* 146–156, 1997.

18. Baserga, R. Oncogenes and the strategy of growth factors. Cell, *79:* 927–930, 1994.

19. Kobayashi, H., Man, S., Graham, C. H., Kapitain, S. J., Teicher, B. A., and Kerbel, R. S. Acquired multicellular-mediated resistance to alkylating agents in cancer. Proc. Natl. Acad. Sci. USA, *90:* 3294–3298, 1993.

20. Rofstad, E. K., Wahl, A., Davies Cde, L., and Brustad, T. Growth characteristics of human melanoma multicellular spheroids in liquid-overlay culture: comparisons with the parent tumour xenografts. Cell Tissue Kinet., *19:* 205–216, 1986.

21. Berlin, O., Samid, D., Donthineni-Rao, R., Akeson, W., Amiel, D., and Woods, V. L, Jr. Development of a novel spontaneous metastasis model of human osteosarcoma transplanted orthotopically into bone of athymic mice. Cancer Res., *53:* 4890–4895, 1993.

22. Samid, D., and Mandler, R. Human Osteosarcoma cells transformed by ras-oncogenes: a new model for *in vivo* studies of pulmonary mtastasis. Clin. Biol., *1:* 21–26, 1989.

23. Voura, E. B., Ramjeesingh, R. A., Montgomery, A. M., and Siu, C. H. Involvement of integrin $\alpha(v)\beta(3)$ and cell adhesion molecule L1 in transendothelial migration of melanoma cells. Mol. Biol. Cell, *12:* 2699–2710, 2001.

Clinical Cancer Research

A Fully Human Antimelanoma Cellular Adhesion Molecule/MUC18 Antibody Inhibits Spontaneous Pulmonary Metastasis of Osteosarcoma Cells *In Vivo*

Eric C. McGary, Amy Heimberger, Lisa Mills, et al.

Clin Cancer Res 2003;9:6560-6566.